

NUMERICAL STUDY OF DAVEY-STEWARTSON I SYSTEMS

JOERG FRAUENDIENER, CHRISTIAN KLEIN, UMAR MUHAMMAD,
AND NIKOLA STOILOV

ABSTRACT. An efficient high precision hybrid numerical approach for integrable Davey-Stewartson (DS) I equations for trivial boundary conditions at infinity is presented for Schwartz class initial data. The code is used for a detailed numerical study of DS I solutions in this class. Localized stationary solutions are constructed and shown to be unstable against dispersion and blow-up. A finite-time blow-up of initial data in the Schwartz class of smooth rapidly decreasing functions is discussed.

1. INTRODUCTION

This paper is concerned with the numerical study of the integrable Davey-Stewartson (DS) I system written in the form

$$(1) \quad \begin{aligned} i\Psi_t + \Psi_{xx} + \Psi_{yy} + 2(\Phi + |\Psi|^2)\Psi &= 0, \\ \Phi_{xx} - \Phi_{yy} + 2|\Psi|_{xx}^2 &= 0, \end{aligned}$$

where indices denote partial derivatives, and where Φ denotes a mean field. In the classification of Ghidaglia and Saut [13], this is an elliptic-hyperbolic equation since the second order operator acting on Ψ in the first equation of (1) is elliptic whereas the one acting on Φ in the second equation of (1) is hyperbolic. Davey-Stewartson systems are of importance in applications since they can be seen as simplifications of the Benney-Roskes [3] and Zakharov-Rubenchik [44] systems, ‘universal’ models for the description of the interaction of short and long waves. These equations have first appeared in the context of water waves [2, 7, 8, 29] in particular in the study of the modulation of plane waves. DS systems also appear in ferromagnetism [30], plasma physics [33], and nonlinear optics [34]. For more details on DS and its applications the reader is referred to [22, 23] where a comprehensive list of references is given. Note that DS I is also interesting from a purely mathematical point of view, since it is a nonlinear dispersive partial differential equation, and since it is one of the few completely integrable equations in two spatial dimensions, see [10, 11]. Local existence results for Cauchy problems with small initial data were proven in [6, 15, 16], and without a smallness assumption in [14].

Date: September 21, 2021.

Key words and phrases. Fourier spectral method, Davey-Stewartson equations, dromions, blow-up.

This work was partially supported by the ANR-FWF project ANuI - ANR-17-CE40-0035, the isite BFC project NAANoD, the ANR-17-EURE-0002 EIPHI and by the European Union Horizon 2020 research and innovation program under the Marie Skłodowska-Curie RISE 2017 grant agreement no. 778010 IPaDEGAN. We thanks J.-C. Saut for helpful discussions and hints.

The hyperbolic form of the second equation in (1) makes it convenient to introduce characteristic coordinates

$$(2) \quad \xi = x - y, \quad \eta = x + y.$$

In these coordinates DS I (1) takes the form of a non-local nonlinear Schrödinger (NLS) equation,

$$(3) \quad i\Psi_t + 2(\partial_\xi^2 + \partial_\eta^2)\Psi + [(\partial_\xi^{-1}\partial_\eta + \partial_\eta^{-1}\partial_\xi)|\Psi|^2]\Psi = 0,$$

where we have formally inverted the d'Alembert operator in the second equation of (1). In order to do so, one has to specify boundary conditions at infinity, a problem analytically discussed in [1] for the multiscales approach to the Kadomtsev-Petviashvili (KP) equation (for a numerical implementation see [24]). In [12] it was shown that *radiating boundary conditions* allow for stable localised traveling waves called *dromions* which appear in the long-time behavior of the solutions to certain initial value problems for DS I. Another possibility applied in this context are vanishing boundary conditions for Ψ in (1) for $\xi, \eta \rightarrow -\infty$ (or $\xi, \eta \rightarrow \infty$). We define the operator ∂_ξ^{-1} (as is standard for the KP equation) via its Fourier symbol,

$$(4) \quad \partial_\xi^{-1} = \mathcal{F}_\xi^{-1} \frac{1}{ik_\xi} = \frac{1}{2} \mathcal{P} \left(\int_{-\infty}^{\xi} - \int_{\xi}^{\infty} \right),$$

where \mathcal{P} denotes the principal value and \mathcal{F}_ξ the Fourier transform in ξ with k_ξ being the dual Fourier variable, and likewise for ∂_η^{-1} . Note that a consequence of this definition is that for $f \in L^1(\mathbb{R})$, one has

$$(5) \quad (\partial_\xi^{-1}f(\xi))(+\infty) = -(\partial_\xi^{-1}f(\xi))(-\infty) = \frac{1}{2} \int_{-\infty}^{\infty} f(\xi)d\xi.$$

These *trivial boundary conditions* will be the only ones studied in this paper.

Numerical studies of DS I solutions have been mainly performed for radiating boundary conditions, see [4, 31, 35, 36, 43]. In this paper we will perform a similar study, but for the trivial boundary conditions (4). Since no explicit solitons are known for this case, we first construct localized stationary solutions numerically and show that they are also exponentially localized. We study the stability of these solutions, which we will also call dromions for simplicity.

In [18, 19] we have shown how to regularize terms of the type (4) arising in the context of D-bar equations with a hybrid approach: we subtract a singular term for which the Fourier transform can be analytically found. The term is chosen in a way that what is left is smooth *within finite numerical precision*, and that its Fourier transform can be numerically computed (we work here with *double precision* which is roughly of the order of 10^{-16}). Note that the terms treated in this way in [18, 19] are less singular (they lead to cusps in the Fourier domain, but are bounded) than the simple poles considered here. Therefore, the regularization approach for DS I is more important than for DS II if high accuracy is to be achieved. We show that we can reach machine precision in the studied examples. Since we want to numerically study blow-up scenarios, an approach of high accuracy as presented here is crucial in order to obtain reliable results.

With this approach, we first construct numerically localized stationary solutions to DS I and propose

Main conjecture (Part I):

The DS I equation has stationary solutions $\Psi(\xi, \eta, t) = Q_\omega(\xi, \eta)e^{i\omega t}$ for $\omega > 0$,

where Q_ω can be chosen to have values in \mathbb{R}^+ . The solutions are exponentially localised.

It is unknown whether these solutions are ground states for the energy (8).

Then we study the time evolution of localised perturbations of these stationary solutions and initial data from the Schwartz class $\mathcal{S}(\mathbb{R}^2)$ of rapidly decreasing smooth functions with a single hump. We find

Main conjecture (Part II):

Initial data $\Psi(\xi, \eta, 0) \in \mathcal{S}(\mathbb{R}^2)$ with a single hump lead to one of the following 3 cases:

- if $\Psi(\xi, \eta, 0) = Q_\omega(\xi, \eta)$, the DS I solution is stationary;
- if the mass $\|\Psi(\xi, \eta, 0)\|_2^2 < m_Q := \|Q\|_2^2$ ($Q := Q_1$), the solution is simply dispersed to infinity;
- if the mass $\|\Psi(\xi, \eta, 0)\|_2^2 > m_Q$, there is a blow-up of the L^∞ norm of Ψ at a finite time t^* such that

$$(6) \quad \Psi(\xi, \eta, t) = \frac{Q(X, Y)}{L(t)} + \tilde{\Psi}(\xi, \eta, t),$$

where X, Y are defined in (12), where $\|\tilde{\Psi}\|_2 < \infty$ for all times, and where

$$(7) \quad L(t) \propto t^* - t.$$

This means that as in the DS II case conjectured in [25], the blow-up is of the type being unstable for standard NLS equations.

The paper is organized as follows: in section 2 we give a brief overview on DS I equations. In section 3 we introduce the hybrid approach to compute the anti-derivatives in ξ and η . Localized stationary solutions to DS I are numerically constructed in section 4. In section 5, we present the time evolution approach and test it at the example of the stationary solution. In section 6, we study the time evolution of these stationary solutions. General localized initial data are studied in section 7. Some concluding remarks are added in section 8.

2. BASIC FACTS

In this section we collect some basic facts on the DS I equation.

We will always study the DS I equation in characteristic coordinates, i.e., in the form (3) of a non-local NLS equation. Note that the sign of the nonlinearity is not important as in the case of the DS II equations, where it distinguishes a focusing and defocusing variant of the equation, see e.g., [22]. For DS I, a change of sign of the nonlinearity can be compensated by a change of sign of either ξ or η and does not affect the behavior of the solutions otherwise.

The DS I equation is completely integrable and thus has an infinite number of formally conserved quantities. In this paper, we will consider the L^2 norm and the energy

$$(8) \quad E = \int_{\mathbb{R}^2} d\xi d\eta \left\{ |\Psi_\xi|^2 + |\Psi_\eta|^2 + \frac{1}{4} \left(\partial_\eta^{-1} |\Psi|^2 \partial_\xi |\Psi|^2 + \partial_\xi^{-1} |\Psi|^2 \partial_\eta |\Psi|^2 \right) \right\}.$$

This form of the energy has been chosen in accordance to the definition of the anti-derivatives (4). It can be shown by direct computation that the energy is conserved in this case.

The DS I equation is expected to have stationary solutions of the form $\Psi(\xi, \eta, t) = Q_\omega(\xi, \eta) e^{i\omega t}$, where $\omega \in \mathbb{R}^+$, and where we get with (3) the following equation for

Q ,

$$(9) \quad -\omega Q + 2(\partial_\xi^2 + \partial_\eta^2)Q + [(\partial_\xi^{-1}\partial_\eta + \partial_\eta^{-1}\partial_\xi)|Q|^2]Q = 0.$$

We are interested in localized solutions to this equation. Note that if the solution $Q := Q_1$ of (9) is known for $\omega = 1$, the solution for arbitrary $\omega > 0$ follows from $Q_\omega = \sqrt{\omega}Q(\sqrt{\omega}\xi, \sqrt{\omega}\eta)$. For the same reasons as for the standard NLS equation, Q can be chosen to be real for localized solutions of this equation. Note that there is an explicit solution to (9) called dromion [27], which reads for $\omega = 1$

$$(10) \quad \tilde{Q} = \frac{1}{4 \cosh \xi/2 \cosh \eta/2 + e^{(\xi+\eta)/2}},$$

if radiating boundary conditions at infinity are used, i.e., if

$$\partial_\xi^{-1} \mapsto \tilde{\partial}_\xi^{-1} + f(\eta), \quad \partial_\eta^{-1} \mapsto \tilde{\partial}_\eta^{-1} + f(\xi),$$

where

$$(11) \quad f(\xi) = \frac{4}{4(1+e^\xi)} + \frac{1}{4(1+2e^\xi)}.$$

It is remarkable that the dromions are exponentially decaying towards infinity in all directions in contrast to the lump solution, the localized stationary solution to DS II which has an algebraic decrease towards infinity. Furthermore, again in contrast to the lump, the dromion is not radially symmetric. Note that it is unknown whether there is an exponentially localised solution to (9) for trivial boundary conditions at infinity.

Below we present some properties of DS I solutions:

- Translation invariance: with $\Psi(t, \xi, \eta)$ a solution to equation (3), also $\Psi(t + t_0, \xi + \xi_0, \eta + \eta_0)$ is a solution, where t_0, ξ_0 , and η_0 are real constants.
- Galilei invariance: with $\Psi(t, \xi, \eta)$ a solution to equation (3), $\Psi(t, \xi - v_\xi t, \eta - v_\eta t) \exp(\frac{i}{2}(v_\xi(\xi - tv_\xi/2) + v_\eta(\eta - tv_\eta/2)))$ with v_ξ, v_η real constants is also a solution. Thus a stationary localized solution can be seen as a soliton to the equation after a Galilei transformation.
- Scaling invariance: with $\Psi(t, \xi, \eta)$ a solution to equation (3), $\lambda \Psi(\lambda^2 t, \lambda \xi, \lambda \eta)$ with $\lambda \in \mathbb{R}/\{0\}$ is also a solution. Note that the L^2 norm of Ψ is invariant under these rescalings. Therefore NLS equations in 2D with a cubic non-linearity are called L^2 critical. It is known that there can be a blow-up in finite time of the L^∞ norm of the solution for smooth initial data with sufficiently large L^2 norm, see [32, 41]. There does not appear to be a theorem on whether DS I or DS II solutions can blow up for generic initial data of sufficient mass.
- Pseudo-conformal invariance: with $\Psi(t, \xi, \eta)$ a solution to (3), also

$$\frac{1}{t} \Psi(1/t, \xi/t, \eta/t) \exp\left(i \frac{\xi^2 + \eta^2}{t}\right)$$

is a solution. This implies together with the translation invariance of DS I that a stationary localized DS I solution under a pseudo-conformal transformation becomes a solution with a blow-up in finite time. This has been used in the context of DS II by Ozawa [37] to construct an explicit blow-up solution. Note that due to the oscillatory terms, the solution will not be in H^1 after a pseudo-conformal transformation even if the original solution

is in L^2 for all t . For standard L^2 critical NLS equations, this blow-up mechanism is unstable, see [41] for references.

The generic blow-up mechanism for NLS solutions is self-similar, which means one uses the above scaling invariance in λ with a time dependent factor $L(t)$ in a *dynamic rescaling*,

$$(12) \quad X = \frac{\xi}{L(t)}, \quad Y = \frac{\eta}{L(t)}, \quad \tau = \int_0^t \frac{dt'}{L^2(t')}, \quad \psi(X, Y, \tau) = L(t)\Psi(\xi, \eta, t).$$

The dynamically rescaled DS I equation (3) then reads

$$(13) \quad i\psi_\tau + i\epsilon a(X\partial_X\psi + Y\partial_Y\psi + \psi) + 2(\partial_X^2 + \partial_Y^2)\psi + [(\partial_X^{-1}\partial_Y + \partial_Y^{-1}\partial_X)|\psi|^2]\psi = 0,$$

where $a = \partial_\tau \ln L$.

In the case of a blow-up, the scaling factor $L(t)$ is chosen in a way to keep certain norms constant during the time-evolution, for instance the L^∞ norm of ψ . If the blow-up is reached for a finite time t^* , then $\lim_{t \rightarrow t^*} L(t) = 0$ and $\lim_{t \rightarrow t^*} \tau = \infty$. For L^2 critical NLS equations, it is expected that $\lim_{t \rightarrow t^*} a(t) = 0$. In this case, equation (13) reduces to the equation for the stationary solution (9) in the limit which would indicate that the blow-up is self-similar with Q giving the blow-up profile. Note, that the generic blow-up rate for L^2 critical NLS is given by (see [32])

$$(14) \quad L(t) \propto \sqrt{\frac{t^* - t}{\ln |\ln(t^* - t)|}}.$$

One of the questions to be addressed in this paper numerically is whether there is blow-up in DS I solutions, and whether it follows the behavior (14) or the pseudo-conformal rate as in DS II, see the conjecture in [25]. To this end we will trace the L^∞ norm of Ψ and the L^2 norm of Ψ_ξ . Both are proportional to $1/L(t)$ and can thus be used to identify the scaling factor $L(t)$.

3. NUMERICAL APPROACH FOR DS I

In this section we briefly describe the numerical approach for the DS I equation, in particular how the antiderivatives in (3) are computed. We will concentrate here on functions in the Schwartz class \mathcal{S} of smooth, rapidly decreasing functions.

The Fourier transform of a 1D function $f(\xi)$ and its inverse are defined via

$$(15) \quad \begin{aligned} \hat{f}(k_\xi) &= \mathcal{F}_\xi f := \int_{\mathbb{R}} e^{-i\xi k_\xi} f(\xi) d\xi, \\ f(\xi) &= \mathcal{F}_\xi^{-1} \hat{f} = \frac{1}{2\pi} \int_{\mathbb{R}} e^{i\xi k_\xi} \hat{f}(k_\xi) dk_\xi. \end{aligned}$$

The 2D Fourier transform of a function $\Phi(\xi, \eta)$ is defined as

$$(16) \quad \begin{aligned} \hat{\Phi}(k_\xi, k_\eta) &= \mathcal{F}_{\xi\eta} \Phi := \int_{\mathbb{R}^2} \Phi(\xi, \eta) e^{-i(\xi k_\xi + \eta k_\eta)} d\xi d\eta, \\ \Phi(\xi, \eta) &= \mathcal{F}_{\xi\eta}^{-1} \hat{\Phi} = \frac{1}{(2\pi)^2} \int_{\mathbb{R}^2} e^{i(\xi k_\xi + \eta k_\eta)} \hat{\Phi}(k_\xi, k_\eta) dk_\xi dk_\eta. \end{aligned}$$

The basic idea of the Fourier spectral method, which we are going to apply here, is to express every function in terms of a Fourier series and approximate the latter via a truncated Fourier series. This is equivalent to approximating the Fourier transform (15) via a *discrete Fourier transform* which can be efficiently computed via a *fast Fourier transform* (FFT). It is well known that the Fourier coefficients of

an analytic periodic function decrease exponentially, and thus the numerical error due to the truncation of the series will also decrease exponentially, see for instance the discussion in [42]. Thus Fourier spectral methods show exponential convergence for analytic functions, sometimes called *spectral convergence*. Here we only consider functions in the Schwartz class which can be efficiently treated as smooth periodic functions on sufficiently large tori within the chosen finite numerical precision (the function and all relevant derivatives have to vanish at the domain boundaries to the chosen numerical precision, here 10^{-16}).

Derivatives of a function $f(\xi) \in \mathcal{S}(\mathbb{R})$, i.e.,

$$f'(\xi) = \mathcal{F}_\xi^{-1}(ik_\xi \hat{f}(k_\xi)),$$

can then be approximated as mentioned above by approximating the standard Fourier transform via a discrete Fourier transform. However, for the antiderivative

$$\partial_\xi^{-1} f(\xi) = \mathcal{F}_\xi^{-1} \left(\frac{1}{ik_\xi} \hat{f}(k_\xi) \right),$$

the singular Fourier symbol will not lead to an exponentially decreasing numerical error if the Fourier transform is approximated via an FFT. Thus we use a hybrid approach, a combination of numerical and analytical techniques, similar to the approach in [20] for the DS II equation. Concretely we write

$$(17) \quad \mathcal{F}_\xi^{-1} \left(\frac{1}{ik_\xi} \hat{f}(k_\xi) \right) = \mathcal{F}_\xi^{-1} \left(\frac{\hat{f}(k_\xi) - \hat{f}(0) \exp(-k_\xi^2/4)}{ik_\xi} \right) + \hat{f}(0) \frac{1}{2} \text{erf}(\xi),$$

where the *error function* $\text{erf}(x)$ is defined as

$$(18) \quad \text{erf}(x) = \frac{2}{\sqrt{\pi}} \int_0^x \exp(-y^2) dy.$$

The error function can be computed to machine precision with the techniques of [26] since the integral is essentially a Hilbert transform in Fourier space. But for simplicity we use the Matlab implementation of the error function here.

The first term on the right hand side of (17) is a smooth function if the limit

$$(19) \quad \lim_{k_\xi \rightarrow 0} \frac{\hat{f}(k_\xi) - \hat{f}(0) \exp(-k_\xi^2)}{ik_\xi} = \hat{f}'(0)$$

is taken into account via de l'Hospital's rule. Since $\hat{f}'(0) = \int_{\mathbb{T}} i\xi f(\xi) d\xi$, this term can be computed again with Fourier techniques (just the sum of $\xi f(\xi)$ sampled on the collocation points). In this way the first term on the right hand side of (17) is in the Schwartz class if $f(\xi)$ is. Thus it can be efficiently computed with Fourier techniques on a large enough torus. Note that a Gaussian was introduced in (17) in order to have an integrand in the Schwartz class to ensure the rapid convergence of the numerical approach. Thus the first term in (17) is computed to machine precision with Fourier techniques whereas the second is obtained with a Matlab algorithm with the same precision.

We illustrate the efficiency of the algorithm for some examples: for a Gaussian $f(\xi) = \exp(-(\xi+1)^2)$ we work with $N = 2^9$ Fourier modes on the interval $10[-\pi, \pi]$. In this case the Fourier coefficients decrease to machine precision. Note that we have considered a shifted Gaussian here in order to have a non-vanishing derivative at the origin in (19). The difference between the error function (times the factor $\sqrt{\pi}/2$) is of the order of 10^{-16} . If we consider with the same numerical parameters

$f(\xi) = \sinh(\xi + 1)/\cosh(\xi + 1)^2$, the Fourier coefficients decrease to the order of 10^{-14} , and the difference to the exact antiderivative $-\text{sech}(\xi + 1)$ is of the same order.

In the context of DS I, we are obviously mainly interested in the accurate numerical computation of the action of the operator $\partial_\xi^{-1}\partial_\eta + \partial_\eta^{-1}\partial_\xi$ on some function in $\mathcal{S}(\mathbb{R}^2)$. To this end we simply apply the above approach in both dimensions. As an example we consider the dromion solution \tilde{Q}_2 for $\omega = 2$ in the case of radiating boundary conditions,

$$(20) \quad |\tilde{Q}_2|^2 = \frac{4}{(4 \cosh(\xi) \cosh(\eta) + \exp(\xi + \eta))^2}.$$

The action of the operator $\partial_\xi^{-1}\partial_\eta + \partial_\eta^{-1}\partial_\xi$ on the dromion can be obviously computed explicitly. We work with $N_\xi = N_\eta = 2^9$ Fourier modes in ξ and η respectively $\partial_\xi^{-1}\partial_\eta + \partial_\eta^{-1}\partial_\xi$ on $10[-\pi, \pi] \times 10[-\pi, \pi]$. The Fourier coefficients of the function (20) can be seen on the left of Fig. 1. They decrease to machine precision. The difference (denoted by err) between the numerically computed action of the operator $\partial_\xi^{-1}\partial_\eta + \partial_\eta^{-1}\partial_\xi$ on (20) and the exact expression can be seen on the right of the same figure. It is as expected of the same order (10^{-15}) as the highest Fourier coefficients.

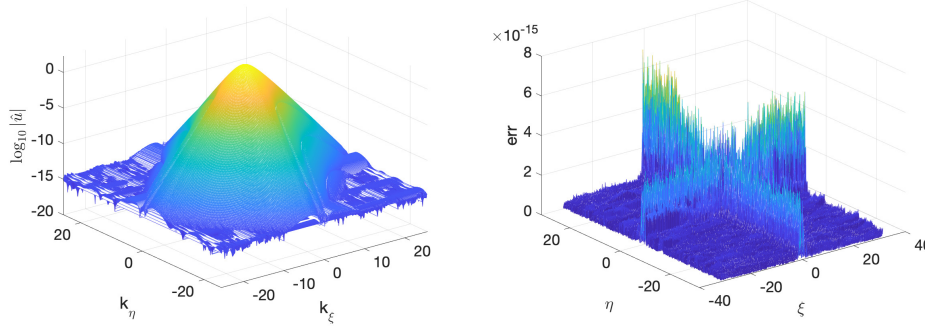


FIGURE 1. The Fourier coefficients of the function (20) on the left, and the difference of the numerically computed action of the operator $\partial_\xi^{-1}\partial_\eta + \partial_\eta^{-1}\partial_\xi$ on (20) and the exact expression on the right.

4. LOCALIZED STATIONARY DS I SOLUTIONS

In this section we numerically construct stationary localized solutions to DS I. This is done with the Fourier discretisation introduced in the previous section for equation (9) with $\omega = 1$. The resulting algebraic equation is then iteratively solved with a Newton-Krylov method.

The task is to find a localized solution to (9) where we restrict ourselves to $\omega = 1$ without loss of generality. In Fourier space, equation (9) reads

$$(21) \quad (1 + 2k_\xi^2 + 2k_\eta^2)\hat{Q} = \mathcal{F}_{\xi\eta} \left([(\partial_\xi^{-1}\partial_\eta + \partial_\eta^{-1}\partial_\xi)|Q|^2]Q \right).$$

As in the previous section, the Fourier transform is approximated via a discrete Fourier transform. This implies that (21) leads to an $N_\xi N_\eta$ dimensional nonlinear equation system of the form $F(\{\hat{Q}\}) = 0$ for \hat{Q} (in an abuse of notation, we denote the discrete Fourier transform as the standard Fourier transform). This system is solved iteratively with a Newton method,

$$(22) \quad \hat{Q}^{(n+1)} = \hat{Q}^{(n)} - \text{Jac}(F)^{-1}|_{\hat{Q}^{(n)}} F(\hat{Q}^{(n+1)}).$$

The action of the Jacobian on F is computed with the Krylov subspace method GMRES [38]. Note that the Jacobian has a finite dimensional kernel because of the translation invariance of the DS I equation. But the iteration converges nonetheless, just the maximum of the resulting solution Q will in general not be at the origin. In the plots below we have shifted the maximum back to the origin.

We use $N_\xi = N_\eta = 2^{10}$ Fourier modes for $(\xi, \eta) \in 20[-\pi, \pi] \times 20[-\pi, \pi]$ and $Q^{(0)} = 6/(4 \cosh(\xi/2) \cosh(\eta/2) + \exp((\xi + \eta)/2))$ as the initial iterate, i.e., 6 times the dromion (10) for radiating boundary conditions. The iteration is stopped once $\|F\|_\infty < 10^{-10}$. The resulting solution can be seen in Fig. 2.

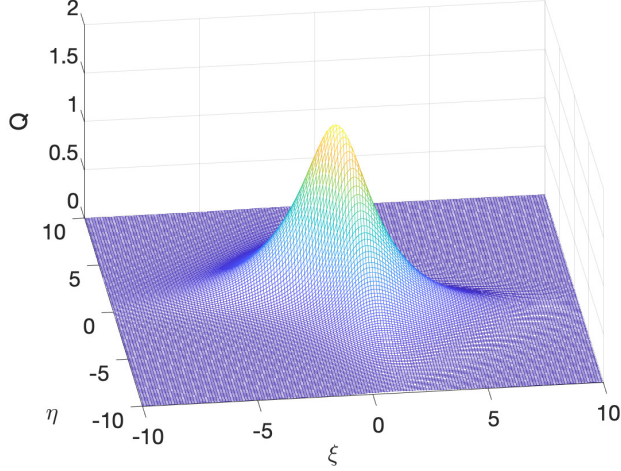


FIGURE 2. Localized stationary solution to DS I (9) for $\omega = 1$.

The solution is again not radially symmetric, but has a symmetry with respect to an exchange of ξ and η as can be clearly seen from the contour plot on the left of Fig. 3. The Fourier coefficients of the solution on the right of the same figure decrease to machine precision and thus indicate that the solutions is numerically well resolved. In fact the numerical parameters have been chosen in a way to ensure this.

Note that the solution is much more peaked than the corresponding one (10) for radiating boundary conditions which can be seen on the left of Fig. 4. In the middle of the same figure, we show the solution of Fig. 2 and (10) on the ξ -axis in one figure. Obviously the solution constructed in this section has a considerably larger maximum (which is why the initial iterate had to be chosen with a factor of 6). It is also more slowly decaying. However, it is also exponentially decaying as can be seen from the logarithmic plot on the right of Fig. 4 on the ξ -axis. We only show

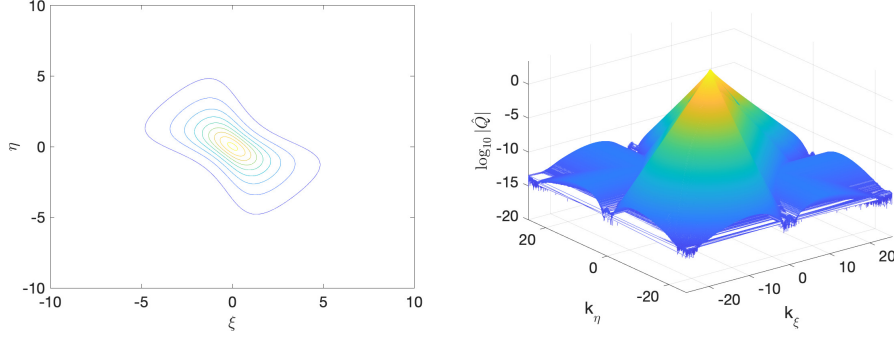


FIGURE 3. Contour plot of the solution in Fig. 2 on the left, and its Fourier coefficients on the right.

the plot on the ξ -axis here, but the same behavior is observed for all values of η , and for the η -dependence for all values of ξ . Thus the stationary solutions to DS I are exponentially localized in contrast to the lumps of DS II which are algebraically decaying, and this not only for radiating boundary conditions. Therefore we will call this solution also dromion in the following even though it is not identical to classical one in (10). Note that the numerical parameters in this section have been chosen in a way that both the solution and its Fourier coefficients decrease to machine precision.

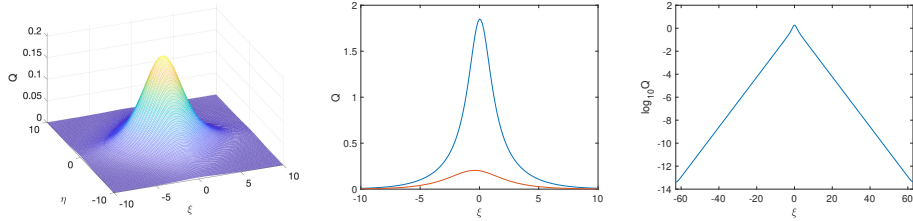


FIGURE 4. Dromion solution (10) for radiating boundary conditions on the left, the same solution on the ξ -axis (red) together with the stationary solution of Fig. 2 (blue) in the middle, and a logarithmic plot of the solution of Fig. 2 on the ξ -axis on the right.

5. TIME EVOLUTION

In this section we outline how the time integration of DS I is handled for the discretisation in the spatial coordinates explained in the previous sections. We discuss how the accuracy of the time integration is controlled and test the code for the example of the stationary solution of the previous section.

We work on $R \times \mathbb{T}_\xi \times \mathbb{T}_\eta$ where $\mathbb{T}_\xi = \mathbb{R}/(2\pi L_\xi \mathbb{Z})$, $\mathbb{T}_\eta = \mathbb{R}/(2\pi L_\eta \mathbb{Z})$. After the FFT discretisation in ξ and η of the previous sections, the DS I equation (3) becomes an $N_\xi N_\eta$ dimensional system of ordinary differential equations of the form (in an abuse of notation, we denote the $N_\xi \times N_\eta$ matrix obtained for $\Psi(\xi, \eta)$ with

the same symbol)

$$(23) \quad \hat{\Psi}_t = \mathcal{L}\hat{\Psi} + \mathcal{N}(\Psi),$$

where

$$(24) \quad \mathcal{L} = -2i(k_\xi^2 + k_\eta^2), \quad \mathcal{N} = i\mathcal{F}_{\xi\eta} \left([(\partial_\xi^{-1}\partial_\eta + \partial_\eta^{-1}\partial_\xi)|\Psi|^2]\Psi \right).$$

The linear part proportional to \mathcal{L} is diagonal and *stiff* since it is quadratic in k_ξ and k_η , which means that explicit time integration schemes are not efficient. For such cases there are many efficient time integration schemes, see for instance the references in [17, 21]. Since it was found in [21] that Driscoll's composite Runge-Kutta method [9] is very efficient for DS equations, we apply it also here.

We use the relative conservation of the mass to control the accuracy in the time integration. Because of unavoidable numerical errors, the numerically computed mass will depend on time even though it is a conserved quantity. Thus $\Delta = \log_{10} |1 - m/m_0|$, where m_0 is the initial mass and m the computed mass can be used to control the accuracy of the temporal discretisation. Generally Δ overestimates the temporal resolution by two orders of magnitude. The relative mass conservation stays well below 10^{-12} throughout most of the runs and sharply increases close to the time t^* of a potential finite time blow-up. Such a jump indicates a loss of precision, and we generally discard results with a value of Δ greater than -3 . Note that we could also use the conserved energy (8) to this end, but the anti-derivatives in (8) make this quantity numerically problematic if resolution in Fourier space is lost near a blow-up. The effect is worse for the energy than for the DS I solution since in the latter, the anti-derivative ∂_ξ^{-1} is multiplied with ∂_η which has a smoothing effect in the space of Fourier coefficients. Thus the energy would underestimate the accuracy near a blow-up which is why we use only mass conservation in the following, where such problems do not appear.

As an example we consider the dromion constructed in the previous section as initial data for DS I. We use $N_t = 10^3$ time steps for $t \leq 1$. The relative conservation of the mass is always to the order of 10^{-15} (the relative energy conservation is of the same order since the solution is fully resolved in Fourier space during the whole computation). Note that the solution is not static, there is a harmonic time dependence. We show the difference between the initial data times $\exp(it)$ and the numerical DS I solution in Fig. 5, on the left the L^∞ norm of the difference between both solutions in dependence of time, on the right the modulus of the difference for $t = 1$ (the difference is always denoted with 'err').

It can be seen that the difference is during the whole computation of the order of 10^{-12} or better which is a remarkable result since it not only shows the accuracy of the time evolution code, but also of the dromion numerically constructed in the previous section. It also shows that the dromion can be stably evolved in time although, as we will show in the following section, it is unstable against perturbations.

6. TIME EVOLUTION OF THE DROMION

In this section we study localized perturbations of the dromion, mainly of the form

$$(25) \quad \Psi(\xi, \eta, 0) = \mu Q, \quad \mu > 0.$$

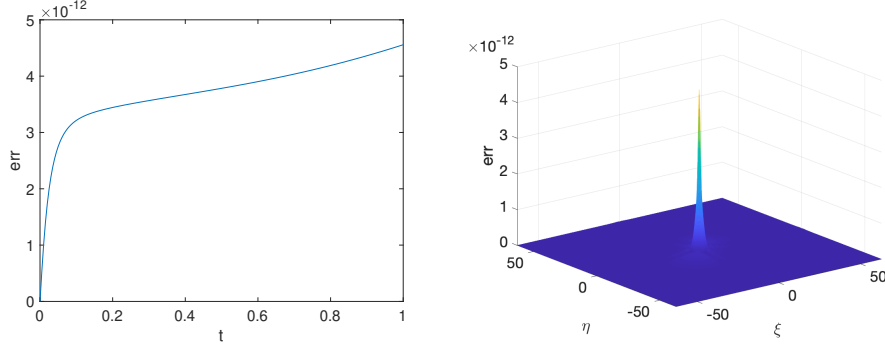


FIGURE 5. Difference of the DS I solution for the initial data $\Psi(\xi, \eta, 0) = Q(\xi, \eta)$ and Qe^{it} , on the left the L^∞ norm of the difference in dependence of time, on the right the difference for $t = 1$.

It is shown that perturbations with a mass smaller than the mass of the dromion are just dispersed, whereas perturbations with a mass larger than the dromion will have a blow-up in finite time.

We first consider the case $\mu = 0.9$ in (25) with $N_\xi = N_\eta = 2^{10}$ Fourier modes and $(\xi, \eta) \in 20[-\pi, \pi] \times 20[-\pi, \pi]$, and with $N_t = 5000$ time steps for $t \leq 5$. In this case the initial hump simply gets dispersed, it gets wider and flatter over time. The solution for $t = 5$ can be seen on the left of Fig. 6. On the right of the same figure the L^∞ norm of the solution appears to be decreasing monotonically. Note that since we approximate a situation on \mathbb{R}^2 with a setting on \mathbb{T}^2 , radiation cannot escape to infinity and thus cannot leave the computational domain. Thus the solution cannot tend to zero even for longer times. However we do not find an indication of a stable structure in DS I solutions for trivial boundary conditions, in contrast to the result in [12] for radiative boundary conditions.

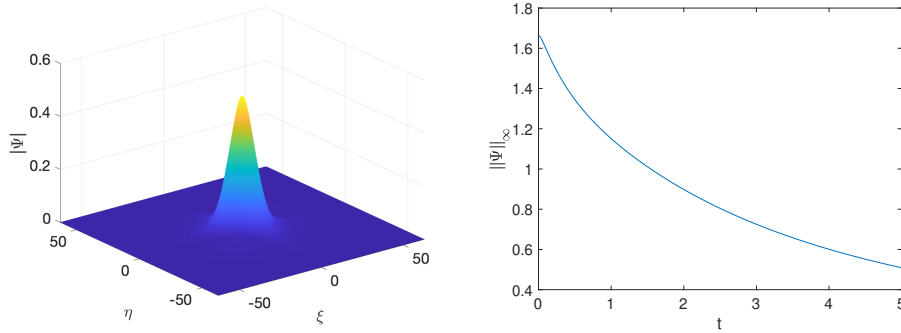


FIGURE 6. Solution to DS I for the initial data $\Psi(\xi, \eta, 0) = 0.9Q$, on the left for $t = 5$, on the right the L^∞ norm in dependence of time.

Then we use the same numerical parameters for the initial data $\Psi(\xi, \eta, 0) = Q - 0.1 \exp(-\xi^2 - \eta^2)$. Note that the mass of these data is roughly $0.96M_Q$ where

M_Q is the mass of the dromion and thus larger than the mass in Fig. 6. We show the solution for $t = 5$ on the left of Fig. 7. Again the initial hump gets just dispersed. This is also confirmed by the L^∞ norm of the solution on the right of the same figure which after some initial oscillation appears to be monotonically decreasing.

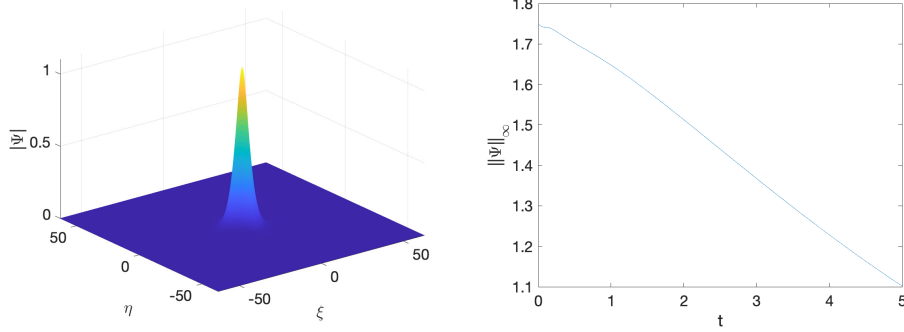


FIGURE 7. Solution to DS I for the initial data $\Psi(\xi, \eta, 0) = Q - 0.1 \exp(-\xi^2 - \eta^2)$, on the left for $t = 5$, on the right the L^∞ norm in dependence of time.

The situation changes considerably if we consider perturbations of the dromion with larger mass. Here the L^∞ norm appears to diverge in finite time which obviously cannot be captured numerically. However we will trace certain norms in this case and fit the found results to the self similar model (12) for blow-up. This allows us to extend data from the region, where the numerical error is still controlled to essentially the full blow-up scenario, i.e., to identify the blow-up time t^* as well as the blow-up rate.

Nonetheless the numerical treatment of a blow-up is a delicate problem. In order to capture the phenomena, we need to make sure to have enough numerical resolution to get close enough to the blow-up in order to identify the mechanism. As before, we use $L_\xi = L_\eta = 20$, but now with $N_\xi = N_\eta = 2^{12}$ Fourier collocation points in each direction. High-index Fourier coefficients, which are used to estimate the space resolution, stay below machine precision throughout the run. In time we use two consecutive runs, one up to $\sim 0.9t^*$, and a second one, with a much finer time step that runs beyond the t^* as estimated from the first run.

In Fig. 6 we show on the left the L^∞ norm of the solution which appears to indicate a finite time blow-up. On the right we trace the quantity Δ indicating the relative conservation of the computed mass. It can be seen to be conserved to better than 10^{-5} during the whole computation.

We show the solution close to the blow-up in Fig. 6.

To study the mechanism of the blow-up, we trace the L^∞ norm of the solution as well as the L^2 norm of the ξ derivative. The fitting of these norms is done for the last several thousand recorded time steps before we start losing temporal resolution. Further we use stabilization of the fit to more precisely judge the data cut off point. Concretely we fit the logarithm of the considered norms, for instance the L^∞ norm according to $\ln \|\Psi\|_\infty = a \ln(t^* - t) + b$ (and similarly for $\|\Psi_\xi\|_2$). The fitting is performed with the algorithm [34] implemented in Matlab as the

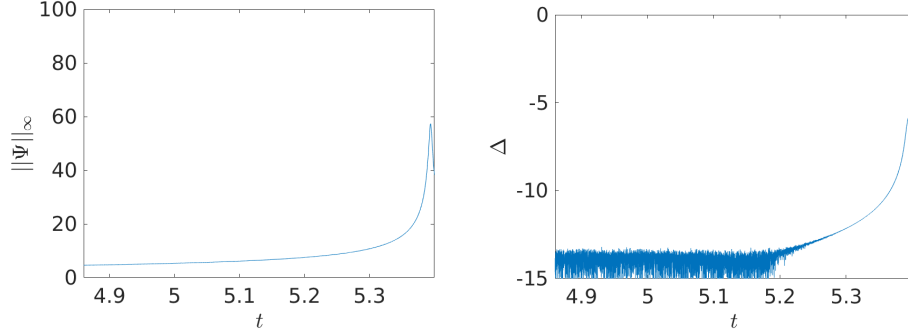


FIGURE 8. DSI solution close to blow-up for initial data $\Psi(\xi, \eta, 0) = 1.1Q$. On the left the evolution of the L^∞ norm of the solution, on the right the conservation of mass $\Delta = \log_{10}(1 - m(t)/m(0))$, which stays below -14 until we get close to the critical time. The fitted blow-up time is $t^* = 5.332$.

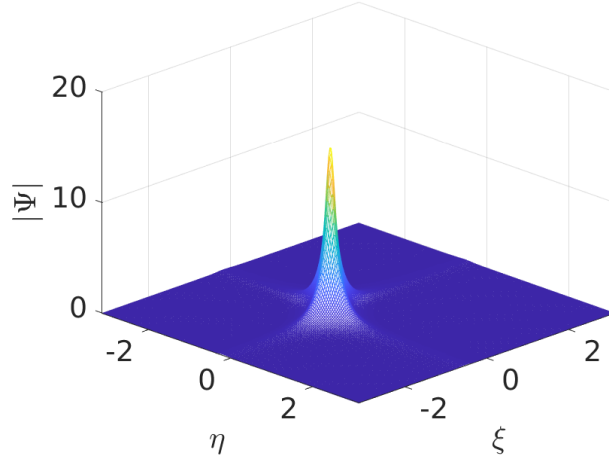


FIGURE 9. DSI solution close to blow-up for initial data $\Psi(\xi, \eta, 0) = 1.1Q$.

command *fminsearch*. For the example with the initial data $1.1Q$, the results can be seen in Fig. 10.

The asymptotic profile of the solution appears to be a scaled dromion according to (12) as can be seen from Fig. 6. The residual is of the order of 10% of the maximum of the fitted solution which shows that one cannot get arbitrarily close to the blow-up numerically, but sufficiently to identify the asymptotic profile.

7. GAUSSIAN INITIAL DATA

In this section, we study more examples from the Schwartz class of functions with a single hump. Since the dromion is not radially symmetric, we concentrate

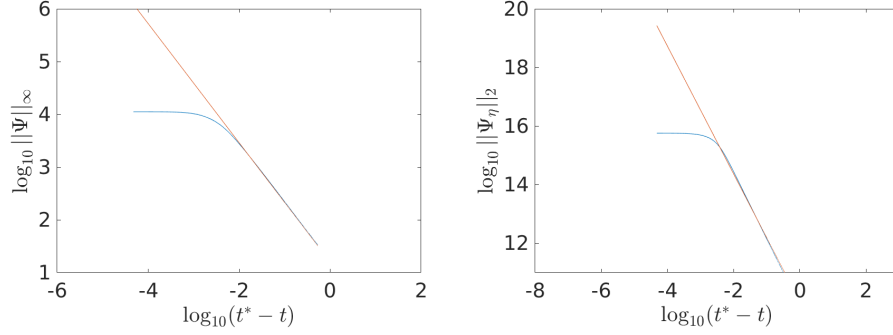


FIGURE 10. Blow-up rate for initial data $\Psi(\xi, \eta, 0) = 1.1Q$. On the left $\|\Psi\|_\infty$, the red lines have the form $a \log_{10}(t^* - t) + b$, with values obtained by fitting the last several thousand points before we lose precision, $a_\infty = 1.13$, $a_{\Psi_x} = 2.18$ and $b_\infty = 1.2$, $b_{\Psi_x} = 10.0$ and $t^* = 0.5394$.

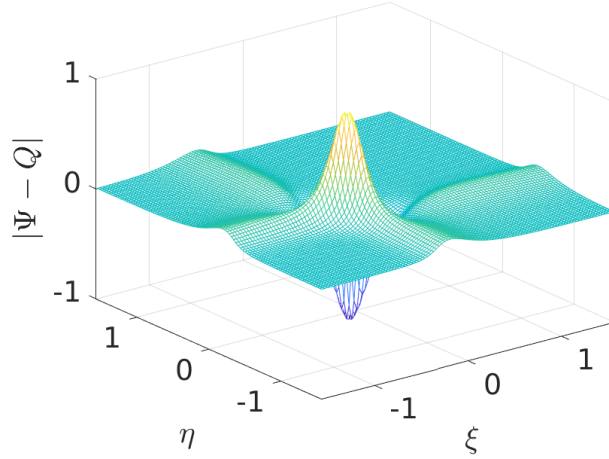


FIGURE 11. Difference of the DS I solution close to blow-up for initial data $\Psi(\xi, \eta, 0) = 1.1Q$ and a scaled dromion.

here on standard Gaussians, i.e., initial data of the form

$$(26) \quad \Psi(\xi, \eta, 0) = \kappa \exp(-\xi^2 - \eta^2), \quad \kappa > 0.$$

Once more we find that initial data with a mass smaller than the dromion will be simply dispersed, whereas initial data with a larger mass will lead to a blow-up in finite time.

First we consider the case $\kappa = 3$ in (26) with a mass of roughly $0.65M_Q$. We use $N_\xi = N_\eta = 2^{10}$ Fourier modes for $(\xi, \eta) \in 10[-\pi, \pi] \times 10[-\pi, \pi]$ and $N_t = 10^3$ time steps for $t \leq 1$. The solution for $t = 1$ is shown on the left of Fig. 12. The initial hump is clearly dispersed. This is also confirmed by the L^∞ norm of the solution on the right of the same figure which after some initial growing appears to decrease monotonically.

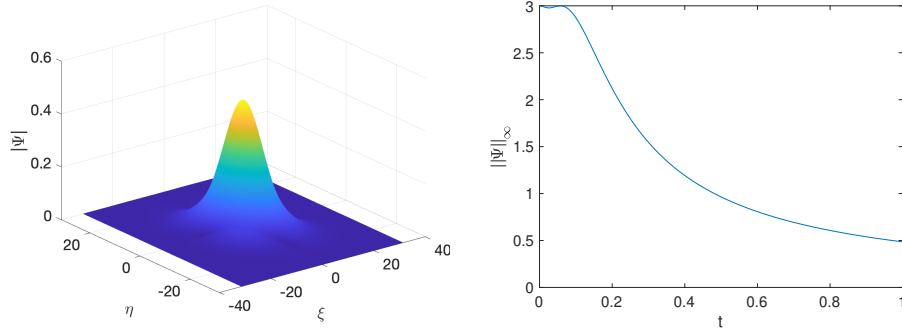


FIGURE 12. Solution to DS I for the initial data $\Psi(\xi, \eta, 0) = 3 \exp(-\xi^2 - \eta^2)$, on the left for $t = 1$, on the right the L^∞ norm in dependence of time.

If we take initial data with a mass larger than the dromion, say $\kappa = 4.5$ in (26) where the mass is roughly $1.45M_Q$, we again seem to get a finite time blow-up. The solution for $t = 0.1570$ in Fig. 7 is already close to the blow-up.

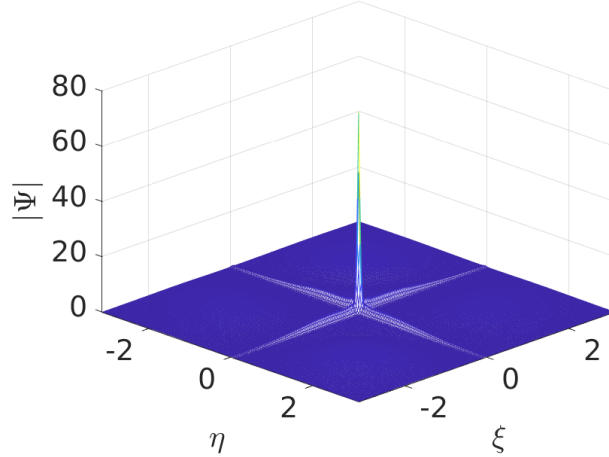


FIGURE 13. DS I solution close to blow-up for Gaussian initial data $\Psi(\xi, \eta, 0) = 4.5e^{-\xi^2 - \eta^2}$.

The L^∞ norm of the solution is monotonically increasing until numerical precision is lost.

A fitting of the L^∞ norm of the solution as well as the L^2 norm of Ψ_ξ as before in Fig. 15 indicates that the blow-up is generic, with blow-up rates

$$\|\Psi\|_\infty \sim |t^* - t|^{-1}, \quad \|\Psi_\xi\|_2^2 \approx |t^* - t|^{-2}.$$

The blow up is self-similar with the profile close to the blow-up being a dynamically rescaled dromion as can be seen from the difference between the solution at

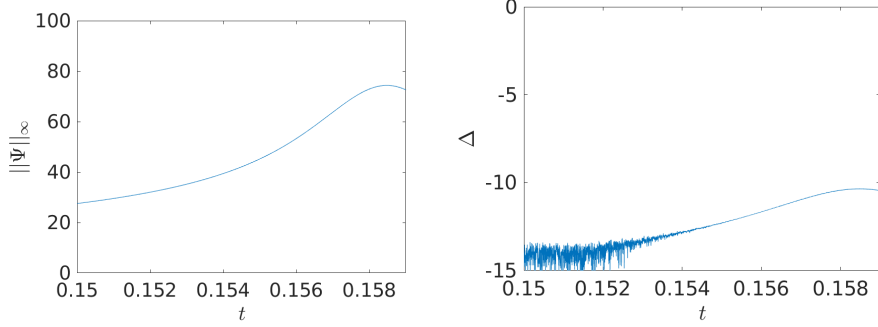


FIGURE 14. DS I solution close to blow-up for Gaussian initial data $\Psi(\xi, \eta, 0) = 4.5e^{-\xi^2 - \eta^2}$. Blow up time at $t = 0.1583$

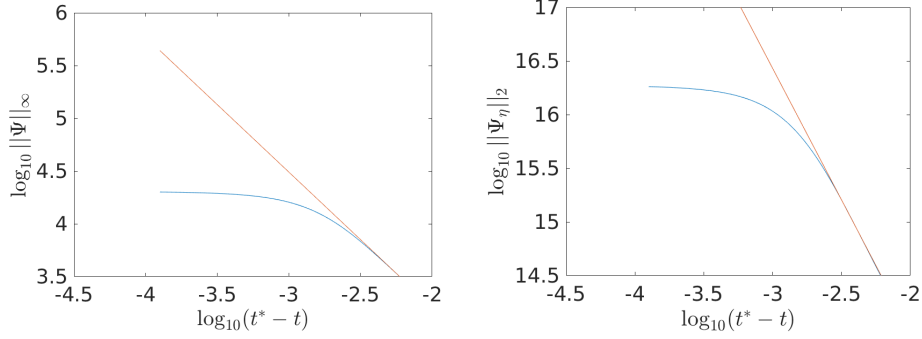


FIGURE 15. Blow-up rate for initial data $\Psi = 4.5e^{-\xi^2 - \eta^2}$, fitting the last several thousand points before we lose precision, $a_\infty = 1.28$, $a_{\Psi_x} = 2.45$ and $b_\infty = 0.65$, $b_{\Psi_x} = 9.08$ and $t^* = 0.1583$.

the final recorded time and rescaled dromion (according to (12) in Fig. 16. The residual is of the order of 10% which once more indicates a good agreement with the model.

8. CONCLUSION

In this paper, we have presented a detailed numerical study of integrable DS I equations with trivial boundary conditions at infinity for initial data from the Schwartz class of rapidly decreasing smooth functions. As in [20] we have presented a hybrid approach based on a Fourier spectral method with an analytic (up to the use of the error function) regularisation of the singular Fourier symbols. With this approach, it was possible to identify a localized stationary solution to DS I which was shown to be exponentially localized as the analytically known dromion for radiative boundary conditions. Strong numerical evidence has been presented that the dromion is unstable against localized perturbations, and that perturbations leading to a smaller mass of the initial data than the dromion mass will be simply dispersed. Perturbations with a larger mass than the dromion will lead to blow-up in finite time. We presented numerical evidence that the blow-up is self-similar

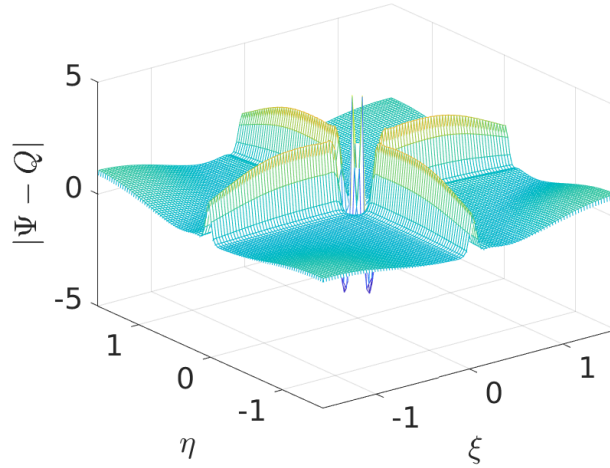


FIGURE 16. Difference of the DS I solution close to blow-up for Gaussian initial data $\Psi(\xi, \eta, 0) = 4.5e^{-\xi^2 - \eta^2}$ and a fitted (according to (12)) dromion.

with the dromion as the asymptotic profile. The same behavior was observed for initial data from the Schwartz class with a single hump.

An interesting question to be studied in the future is whether dromions also exist for non-integrable generalisations of DS I and DS II, and whether a blow-up is still observed in such cases. A first study of these questions for DS II was presented in [23] and should also be redone with the methods of [20].

REFERENCES

- [1] M.J. Ablowitz, S.V. Manakov and C.L. Schultz, On the boundary conditions of the Davey-Stewartson equation, *Phys. Lett. A* 148 (1990) 50-52.
- [2] M.J. Ablowitz and H. Segur, On the evolution of packets of water waves, *J. Fluid Mech.* 92 (1979), 691-715.
- [3] D.J. Benney and G.J. Roskes, Waves instabilities, *Stud. Appl. Math.* 48 (1969), 377-385.
- [4] C. Besse, C.H. Bruneau, Numerical study of elliptic-hyperbolic Davey-Stewartson system: dromions simulation and blow-up, *Math. Mod. and Meth. in Appl. Sciences* 8, No. 8 (1998), 1363-1386
- [5] C. Besse, N. Mauser, and H. Stimming, Numerical Study of the Davey-Stewartson System, *Math. Model. Numer. Anal.*, 38 (2004), pp. 1035-1054.
- [6] H. Chihara, The initial value problem for the elliptic-hyperbolic Davey-Stewartson equation, *J.Math.Kyoto Univ.* 39 no 1 (1999), 41-66.
- [7] A. Davey and K. Stewartson, On Three-dimensional Packets of Surface Waves, *Proc. R. Soc. Lond. A.*, 338 (1974), pp. 101-110.
- [8] V.D. Djordjevic and L.G. Redekopp, On two-dimensional packets of capillary-gravity waves, *J. Fluid Mech.* 79 (1977), 703-714.
- [9] T. Driscoll, A composite Runge-Kutta Method for the spectral Solution of semilinear PDEs, *Journal of Computational Physics*, 182 (2002), pp. 357-367.
- [10] Fokas AS. 1983 On the inverse scattering of first order systems in the plane related to nonlinear multidimensional equations. *Phys. Rev. Lett.* 51, 3-6. (doi:10.1103/PhysRevLett.51.3) 47.
- [11] Fokas AS, Ablowitz MJ. 1983 On a method of solution for a class of multi-dimensional nonlinear evolution equations. *Phys. Rev. Lett.* 51, 7-10. (doi:10.1103/PhysRevLett.51.7)

- [12] A.S. Fokas and P.M. Santini, Dromions and a boundary value problem of the Davey-Stewartson I equation, *Physica D* 44 (1990) 99-130.
- [13] J.-M. Ghidaglia and J.-C. Saut, On the initial value problem for the Davey-Stewartson systems, *Nonlinearity*, 3, (1990), 475-506.
- [14] N. Hayashi, Local existence in time of solutions to the elliptic-hyperbolic Davey-Stewartson system without smallness condition on the data, *J. Analyse Mathématique* 73, (1997), 133-164.
- [15] N. Hayashi and H. Hirota, Global existence and asymptotic behavior in time of small solutions to the elliptic-hyperbolic Davey-Stewartson system, *Nonlinearity* 9 (1996), 1387-1409.
- [16] N. Hayashi and J.-C. Saut, Global existence of small solutions to the Davey-Stewartson and the Ishimori systems, *Diff. Int. Equations* 8 (7) (1995), 1657-1675.
- [17] C. Klein, Fourth order time-stepping for low dispersion Korteweg-de Vries and nonlinear Schrödinger equation, *ETNA Vol. 29* 116-135 (2008).
- [18] C. Klein and K. McLaughlin, Spectral approach to D-bar problems, *Comm. Pure Appl. Math.*, DOI: 10.1002/cpa.21684 (2017)
- [19] C. Klein, K. McLaughlin, N. Stoilov, Spectral approach to the scattering map for the semi-classical defocusing Davey-Stewartson II equation, *Physica D*, doi.org/10.1016/j.physd.2019.05.006
- [20] C. Klein, K. McLaughlin, N. Stoilov, High precision numerical approach for Davey-Stewartson II type equations for Schwartz class initial data, *Proc. Royal Soc. A* 476, <https://doi.org/10.1098/rspa.2019.0864>
- [21] C. Klein and K. Roidot, Fourth order time-stepping for Kadomtsev-Petviashvili and Davey-Stewartson equations, *SIAM J. Sci. Comput.*, 33(6), 3333-3356. DOI: 10.1137/100816663 (2011).
- [22] C. Klein and J.-C. Saut, *IST versus PDE, a comparative study*, in *Hamiltonian Partial Differential Equations and Applications* ed. by P. Guyenne, D. Nicholls, C. Sulem, *Fields Inst. Commun.* 75, 338-449 (2015), DOI: 10.1007/978-1-4939-2950-4
- [23] C. Klein and J.-C. Saut, *A numerical approach to Blow-up issues for Davey-Stewartson II type systems*, *Comm. Pure Appl. Anal.* 14:4, 1443-1467 (2015)
- [24] C. Klein, C. Sparber and P. Markowich, *Numerical study of oscillatory regimes in the Kadomtsev-Petviashvili equation*, *J. Nonl. Sci. Vol.* 17(5), 429-470 (2007).
- [25] C. Klein and N. Stoilov, A numerical study of blow-up mechanisms for Davey-Stewartson II systems, *Stud. Appl. Math.*, DOI : 10.1111/sapm.12214 (2018)
- [26] C. Klein, N. Stoilov, Multi-domain spectral approach for the Hilbert transform on the real line, *SN Partial Differential Equations and Applications* (2:36) (2021) <https://doi.org/10.1007/s42985-021-00094-8>
- [27] Konopelchenko, B.G. (1993) *Solitons in Multidimensions*, World Scientific, Singapore.
- [28] Lagarias, J. C., J. A. Reeds, M. H. Wright, and P. E. Wright. Convergence Properties of the Nelder-Mead Simplex Method in Low Dimensions. *SIAM Journal of Optimization*. Vol. 9, Number 1, 1998, pp. 112-147.
- [29] D. Lannes, *Water waves: mathematical theory and asymptotics*, *Mathematical Surveys and Monographs*, vol 188 (2013), AMS, Providence.
- [30] H. Leblond, Electromagnetic waves in ferromagnets, *J. Phys. A* 32 (45) (1999), 7907-7932.
- [31] M. McConnell, A.S. Fokas, B. Pelloni, Localised coherent solutions of the DSI and DSII equations—a numerical study, *Math. Comp. Sim.* 69 (2005) 424-438
- [32] F. Merle, P. Raphael, On universality of blow-up profile for L^2 critical nonlinear Schrödinger equation, *Invent. math.* **156**, 565-672 (2004)
- [33] S.L. Musher, A.M. Rubenchik and V.E. Zakharov, Hamiltonian approach to the description of nonlinear plasma phenomena, *Phys. Rep.* 129 (5) (1985), 285-366.
- [34] A. Newell and J.V. Moloney, *Nonlinear Optics*, Addison-Wesley (1992).
- [35] K. Nishinari, T. Yajima, Numerical analyses of the collision of localised structures in the Davey-Stewartson equations, *Phys. Rev. E* 51 (1995) 4986-4993.
- [36] K. Nishinari, T. Yajima, T. Nakao, Time Evolution of Gaussian Type Initial Conditions Associated With The Davey-Stewartson Equations, *J. Phys. A: Math. Gen.* 29 (1996) 4237-4245.
- [37] T. Ozawa, Exact Blow-Up Solutions to the Cauchy Problem for the Davey-Stewartson Systems, *Proc. R. Soc. Lond. A.*, 436 (1992), pp. 345-349.
- [38] Y. Saad and M. Schultz, GMRES: a generalized minimal residual algorithm for solving non-symmetric linear systems, *SIAM J. Sci. Comput.* 7 (1986), 856-869.

- [39] E.I. Schulman, On the integrability of equations of Davey-Stewartson type, Theor. Math. Phys. 56 (1983), 131-136.
- [40] G.C. Papanicolaou, C. Sulem, P.L. Sulem and X.P. Wang, Focusing singularities of Davey-Stewartson equations for gravity-capillary waves, preprint
- [41] C. Sulem, P.-L. Sulem, *The nonlinear Schrödinger equation. Self-focusing and wave-collapse*. Springer, 1999.
- [42] L. N. Trefethen, Spectral Methods in Matlab, SIAM, Philadelphia, PA, 2000.
- [43] P. White and J. Weideman, Numerical Simulation of Solitons and Dromions in the Davey-Stewartson System, Math. Comput. Simul., 37 (1994), pp. 469-479.
- [44] V. E. Zakharov and A. M. Rubenchik, Nonlinear interaction of high-frequency and low frequency waves, Prikl. Mat. Techn. Phys., (1972), 84-98.
- [45] V. E. Zakharov and, E. I. Schulman, Degenerate dispersion laws, motion invariants and kinetic equations, Physica 1D (1980), 192-202.
- [46] V. E. Zakharov and, E. I. Schulman, Integrability of nonlinear systems and perturbation theory, in What is integrability? (V.E. Zakharov, ed.), (1991), 185-250, Springer Series on Nonlinear Dynamics, Springer-Verlag.

(J. Frauendiener) DEPARTMENT OF MATHEMATICS AND STATISTICS, UNIVERSITY OF OTAGO,
P.O. BOX 56, DUNEDIN 9010, NEW ZEALAND
Email address: joergf@maths.otago.ac.nz

(C. Klein) INSTITUT DE MATHÉMATIQUES DE BOURGOGNE 9 AVENUE ALAIN SAVARY, BP 47870,
21078 DIJON CEDEX
Email address: christian.klein@u-bourgogne.fr

(U. Muhammad) INSTITUT DE MATHÉMATIQUES DE BOURGOGNE, UMR 5584, UNIVERSITÉ DE
BOURGOGNE-FRANCHE-COMTÉ, 9 AVENUE ALAIN SAVARY, 21078 DIJON CEDEX, FRANCE
Email address: umarmuhddaouda@gmail.com

(N. Stoilov) INSTITUT DE MATHÉMATIQUES DE BOURGOGNE, UMR 5584, UNIVERSITÉ DE BOURGOGNE-
FRANCHE-COMTÉ, 9 AVENUE ALAIN SAVARY, 21078 DIJON CEDEX, FRANCE
Email address: Nikola.Stoilov@u-bourgogne.fr